



RESEARCH ARTICLE

Temporal variability of regional intrinsic neural activity in drug-naïve patients with obsessive–compulsive disorder

Jing Liu^{1,2} | Xuan Bu^{1,2} | Xinyu Hu^{1,2} | Hailong Li^{1,2} | Lingxiao Cao^{1,2} |
Yingxue Gao^{1,2} | Kaili Liang^{1,2} | Lianqing Zhang^{1,2} | Lu Lu^{1,2} | Xinyue Hu^{1,2} |
Yanlin Wang^{1,2} | Qiyong Gong^{1,2}  | Xiaoqi Huang^{1,2} 

¹Huaxi MR Research Center (HMRRC), Functional and Molecular Imaging Key Laboratory of Sichuan Province, Department of Radiology, West China Hospital, Sichuan University, Chengdu, China

²Psychoradiology Research Unit of the Chinese Academy of Medical Sciences, West China Hospital of Sichuan University, Chengdu, Sichuan, China

Correspondence

Xiaoqi Huang, Huaxi MR Research Center (HMRRC), Functional and Molecular Imaging Key Laboratory of Sichuan Province, Department of Radiology, West China Hospital, Sichuan University, No. 37 Guo Xue Xiang, Chengdu 610041, China.
Email: julianahuang@163.com

Funding information

National Natural Science Foundation of China, Grant/Award Number: 81671669; Science and Technology Project of Sichuan Province, Grant/Award Number: 2017JQ0001; Science and Technology Project of Chengdu City, Grant/Award Number: 2019-YF05-00509-SN

Abstract

Obsessive–compulsive disorder (OCD) displays alterations in regional brain activity represented by the amplitude of low-frequency fluctuation (ALFF), but the time-varying characteristics of this local neural activity remain to be clarified. We aimed to investigate the dynamic changes of intrinsic brain activity in a relatively large sample of drug-naïve OCD patients using univariate and multivariate analyses. We applied a sliding-window approach to calculate the dynamic ALFF (dALFF) and compared the difference between 73 OCD patients and age- and sex-matched healthy controls (HCs). We also utilized multivariate pattern analysis to determine whether dALFF could differentiate OCD patients from HCs at the individual level. Compared with HCs, OCD patients exhibited increased dALFF mainly within regions of the cortical–striatal–thalamic–cortical (CSTC) circuit, including the bilateral dorsal anterior cingulate cortex, medial prefrontal cortex and striatum, and right dorsolateral prefrontal cortex (dlPFC). Decreased dALFF was identified in the bilateral inferior parietal lobule (IPL), posterior cingulate cortex, insula, fusiform gyrus, and cerebellum. Moreover, we found negative correlations between illness duration and dALFF values in the right IPL and between dALFF values in the left cerebellum and Hamilton Depression Scale scores. Furthermore, dALFF can distinguish OCD patients from HCs with the most discriminative regions located in the IPL, dlPFC, middle occipital gyrus, and cuneus. Taken together, in the current study, we demonstrated a characteristic pattern of higher variability of regional brain activity within the CSTC circuits and lower variability in regions outside the CSTC circuits in drug-naïve OCD patients.

KEYWORDS

dynamic amplitude of low-frequency fluctuation, multivariate pattern analysis, obsessive–compulsive disorder, resting-state fMRI

Jing Liu and Xuan Bu contributed equally to this work.

This is an open access article under the terms of the Creative Commons Attribution-NonCommercial License, which permits use, distribution and reproduction in any medium, provided the original work is properly cited and is not used for commercial purposes.

© 2021 The Authors. *Human Brain Mapping* published by Wiley Periodicals LLC.

1 | INTRODUCTION

Obsessive-compulsive disorder (OCD) is a disabling psychiatric disorder with an approximate lifetime prevalence of 2–3%. Patients with OCD are characterized by recurrent unwanted thoughts, images, or impulses (obsessions) and repetitive behaviors (compulsions) (Stein et al., 2019), which are associated with substantial global disability. Although multiple advances have been made in the exploration of neural deficits related to OCD, the precise underlying neural mechanisms of OCD remain unclear.

One neuropathology hypothesis of OCD is that it is caused by the disruption of large-scale functional brain networks, particularly three networks (the frontoparietal network, default mode network, and salience network), which together are called the triple network model and underlie the pathophysiology of OCD (Gürsel, Avram, Sorg, Brandl, & Koch, 2018). Nevertheless, dysfunction of other networks, such as the visual and cerebellar networks, has also been discovered (Reggente et al., 2018; Xu et al., 2019). More recently, the temporal dynamic properties of functional network connectivity in the resting state have gained increased attention because a more thorough understanding of the brain's function can be obtained through its analysis (Liao et al., 2019). The aberrant dynamic functional network connectivity patterns emerging from this analysis have been identified as important features of many psychiatric disorders, such as schizophrenia (Wang, Zhang, Sun, Hu, & Chen, 2016), major depressive disorder (MDD) (Qiu et al., 2018) and OCD (Gürsel et al., 2020; Liu et al., 2020).

The brain functional network is usually described as the functional connectivity between regions and the activity strength of the local brain region, particularly the hub regions (Hou et al., 2014). A previous study demonstrated that local neural activity itself fluctuates substantially and is correlated with dynamic functional network connectivity (Fu et al., 2018). Therefore, focusing only on the time-varying patterns of functional connectivity is insufficient, and the investigation of dynamic changes in regional brain activity holds promise to provide information about regional alterations within a network and can help researchers understand the neuropathological mechanism of mental diseases (Fan et al., 2017).

The amplitude of low-frequency fluctuation (ALFF) has been proven to be an effective and reliable parameter for evaluating local intrinsic brain activity (Zang et al., 2007), which is closely associated with mental state and cognitive processes (Raichle & Snyder, 2007). ALFF represents a potential relationship to the brain's glucose metabolism (Aiello et al., 2015) and morphology (Liao et al., 2016). Alterations in ALFF in cerebral regions that comprise the cortical-striatal-thalamic-cortical (CSTC) circuits and other regions, such as the parietal gyrus, middle occipital gyrus (MOG), middle temporal gyrus (MTG), and cerebellum, have also been implicated in OCD patients (Fan et al., 2017; Hou et al., 2012). Although these altered spontaneous neuronal activities improve our understanding of the pathophysiologic characteristics of OCD, the aforementioned ALFF measures are static throughout the entire scan, ignoring the characteristics of dynamic changes of intrinsic brain activity over time in patients with OCD.

In our previous study, we demonstrated alterations in static ALFF among patients with drug-naïve OCD and found that ALFF had the best performance in discriminating OCD from healthy controls (HCs) among four resting-state functional magnetic resonance imaging (rs-fMRI) parameters (Bu et al., 2019). Thus, in the current study, we mainly focused on the temporal variability of ALFF and its potential role in classification. Because medication and other treatments have been proven to have effects on brain structure (Benedetti et al., 2013) and function (Yin et al., 2018), we recruited only patients who had never received systematic treatment before to exclude these confounding factors (Boedhoe et al., 2018), and thus reveal the temporal variability of intrinsic cerebral activity directly related to disease pathology.

2 | MATERIALS AND METHODS

2.1 | Participants

The study was approved by the Ethics Committee of the West China Hospital, Sichuan University, and written informed consent was obtained from each participant. We recruited 74 OCD patients who had never received medication or systematic psychotherapy and 76 HCs. Among them, 54 OCD patients and 54 HCs were the same as our previous analysis (Bu et al., 2019). All the subjects were right-handed individuals and native Chinese speakers. OCD patients were recruited from the Mental Health Center, West China Hospital, Sichuan University. The diagnosis of OCD was made by two experienced clinical psychiatrists based on the Structured Clinical Interview for DSM-IV Axis I Disorders (SCID). The Yale-Brown Obsessive-Compulsive Scale (Y-BOCS) was used to rate the severity of OCD symptoms, whereas the 14-item Hamilton Anxiety Scale (HAMA) and 17-item Hamilton Depression Scale (HAMD) were used to assess accompanying anxiety and depression symptoms.

These patients had not received any prior psychiatric medications for various reasons, mainly because of (a) a lack of understanding or recognition of the severity of mental illness and (b) poor socioeconomic conditions that limited travel and search for medical care in rural areas. As a result of these factors, each patient had been sheltered in the home without medical care through the course of the illness.

Seventy-six HCs were recruited via a poster and were screened by two experienced psychiatrists using the SCID (nonpatient edition) to confirm the current absence of psychiatric and neurological illness as well as the absence of a history of psychiatric illness among first-degree relatives.

The exclusion criteria, applied to both OCD patients and HCs, included the following: (a) the existence of neurological diseases or other mental disorders; (b) any history of cardiovascular diseases, metabolic disorders, or major physical illness; (c) history of previous substance abuse for any drugs or alcohol; (d) pregnancy and (e) participants younger than 18 years or older than 60 years.

2.2 | Image acquisition

All the participants were scanned using a 3.0-T MRI system (EXCITE; General Electric, Milwaukee, WI) with an eight-channel phase-array head coil. Before scanning, the participants were instructed to stay awake with their eyes closed. Foam pads were used to reduce head motion, and earplugs were used to attenuate scanner noise.

The rs-fMRI images were obtained using a gradient-echo echo-planar imaging sequence with the following parameters: time repetition (TR) = 2,000 ms, time echo (TE) = 30 ms, flip angle = 90°, slice thickness = 5 mm with no slice gap, field of view (FOV) = 240 × 240 mm², matrix size = 64 × 64, 30 axial slices, and 200 volumes in each run.

High-resolution, T1-weighted images were acquired using a volumetric three-dimensional spoiled gradient recall sequence with the following parameters: TR = 8.5 ms, TE = 3.4 ms, flip angle = 12°, axial slice thickness = 1.0 mm, FOV = 240 × 240 mm², matrix size = 256 × 256, and number of coronal slices = 156.

2.3 | Image preprocessing

The data were processed using the Data Processing Assistant for Resting-State fMRI (DPARSFA; <http://rfmri.org/dpabi>, version 4.4) (Yan, Wang, Zuo, & Zang, 2016). For each subject, the first 10 volumes were discarded to ensure signal stabilization. The remaining 190 rs-fMRI images were corrected for acquisition time intervals between slices and head motion between volumes.

After these corrections, the structural image was coregistered to the mean functional image of each participant, and the transformed structural image was segmented into gray matter, white matter, and cerebrospinal fluid. Based on these segmented images, the Diffeomorphic Anatomical Registration Through Exponentiated Lie algebra tool (Ashburner, 2007) was used to compute transformations from the individual native space to the Montreal Neurological Institute space. To remove the head-motion artifacts, we adopted the regressors of the Friston 24-parameter model (Friston, Williams, Howard, Frackowiak, & Turner, 1996), which was demonstrated to be superior to the 6-parameter model (Yan et al., 2013). Furthermore, we regressed out covariates including the cerebrospinal fluid signal and white matter signal to minimize the effects of nonneuronal blood oxygen level-dependent fluctuations.

Thereafter, the linear trend in the fMRI data were removed to decrease the impact of high-frequency physiological noise and very low-frequency drift.

2.4 | Quality control for head motion

We used stringent criteria to minimize the effects of head motion on dynamic ALFF (dALFF). Here, we only selected participants with relatively low head motion, as assessed using mean framewise displacement (derived from Jenkinson's formula (Jenkinson, Bannister,

Brady, & Smith, 2002)) (criteria: mean FD < 0.2 mm). This method greatly reduces motion-induced artifacts when combined with various motion correction strategies (Power, Barnes, Snyder, Schlaggar, & Petersen, 2013; Satterthwaite et al., 2013). Additionally, this threshold has been used in recent dynamic studies to rigorously control head motion (Denkova, Nomi, Uddin, & Jha, 2019; Yan, Yang, Colcombe, Zuo, & Milham, 2017). We also calculated three translational parameters and three rotational parameters obtained from the realignment steps for each subject. The rs-fMRI images meeting the criteria of <1.5 mm of spatial movement and <1.5° of rotation in any direction were retained. Because of the necessary contiguous time points in dALFF analysis, we did not perform scrubbing, which alters the temporal structure of the data (Yan et al., 2013).

After these head motion controls, four of the subjects (three HCs and one OCD patient) were excluded.

2.5 | dALFF calculation

The dALFF analysis was performed using the temporal dynamic analysis toolkits based on Data Processing and Analysis of Brain Imaging (DPABI; <http://rfmri.org/dpabi>, version 3.1) (Yan, Wang, Zuo, & Zang, 2016). A sliding-window approach was performed to characterize the dALFF throughout the whole brain.

The window length is an open but important parameter. Previous studies demonstrated that a window length of 50 TRs (100 s) is the optimal parameter to maintain the balance between capturing rapidly shifting dynamic activity (with shorter windows) and achieving reliable estimates of brain activity (with longer windows) (Cui et al., 2020; Liao et al., 2019). Thus, we selected 50 TRs as the sliding window length and 1 TRs as the step size to calculate the dALFF of each participant. The time series of each participant was divided into 141 windows, and the ALFF map was computed within each window.

Specifically, the time series in each window was first converted to the frequency domain with a fast Fourier transform, and the power spectrum was obtained. The sum of the amplitudes in the low-frequency bands (0.01–0.08 Hz) was calculated, and the averaged square root of the power in the above frequency windows at each voxel represents the ALFF measured value. The SD of the ALFF at each voxel across 141 windows was calculated to assess the temporal variability of the ALFF, which is defined as dALFF. For standardization, the dALFF of each voxel was divided by the global mean dALFF values within a gray matter mask. Finally, the mean normalized dALFF maps were spatially smoothed using an isotropic Gaussian kernel of 8 mm full-width at half-maximum.

2.6 | Univariate group comparison

Two-sample *t* tests were performed to assess the group differences in dALFF between the OCD patients and HCs, with age, sex and mean FD as covariates. We utilized a statistical height threshold of $p_{\text{uncorr}} < .001$ at the voxel level and a false discovery rate (FDR)

correction of $p_{\text{corr}} < .05$ at the cluster level for multiple comparison correction. All statistical analyses were performed using SPM12 software (<http://www.fil.ion.ucl.ac.uk/spm/software/spm12/>).

2.7 | Correlation analysis

To examine the association between alterations of dALFF and clinical symptoms, we performed Pearson's correlation analyses between the illness duration, Y-BOCS scores, obsessions, compulsions, HAMA scores, and HAMD scores and the dALFF values from regions showing group differences.

2.8 | Multivariate pattern analysis

Multivariate pattern analysis (MVPA) is a useful approach based on a machine learning algorithm that can classify patients and healthy subjects at the individual level (Vieira, Pinaya, & Mechelli, 2017) and has shown promise for making diagnostic predictions in psychiatric disorders (Huang, Gong, Sweeney, & Biswal, 2019). In the present study, we used the linear support vector machine (SVM) as implemented in the PRoNTTo toolbox (<http://www.mlnl.cs.ucl.ac.uk/pronto/prtsoftware.html>, Version 2.1.1) (Ashburner et al., 2012) to distinguish patients with OCD and HCs on the basis of whole-brain dALFF maps.

In SVM, individual brain scans were treated as points located at high-dimensional space defined by the dALFF map in the preprocessed images. In this high-dimensional space, a linear decision boundary was defined by a "hyperplane" that separated the individual brain scans according to a class label (i.e., OCD patients vs. HCs). The optimal hyperplane was computed based on the whole multivariate pattern of the dALFF map across each image.

The considered algorithm is based on the SVM model, which includes a soft-margin parameter C . This hyperparameter penalizes more (large values of C) or less (small values of C) misclassifications during training and affects the resulting decision boundary (Schrouff, Mourão-Miranda, Phillips, & Parvizi, 2016). Thus, a nested cross-validation (CV) with hyperparameter optimization was used in our study. In this case, there are two loops in the CV scheme. The inner CV selected the value of C leading to the highest model performance, and the outer CV estimated the performance on a test set using the selected value of C . We used soft-margin hyperparameter optimization with the best configuration among $C = 0.01, 0.1, 1, 10,$ and 100 .

For the outer loop, we adopted 10-fold CV on subject per group out method to evaluate classification performance, which is preferred because the training sets have less overlap (resulting in less variance in the test error), and the approach is suitable for our paired samples (Halai, Woollams, & Lambon Ralph, 2020). Specifically, the dataset was randomly divided into 10 folds for each group at a time, one pair of folds (one OCD fold and one HCs fold) was selected as the testing set, and the remaining nine pairs of folds were used as training sets. This procedure for the outer loop was repeated 10 times to ensure that every fold had a chance to become a test dataset. The inner loop adopted the same

CV scheme as the external loop since it had fewer folds and reduced the computational time (Youssofzadeh, McGuinness, Maguire, & Wong-Lin, 2017). A detailed description of the method was displayed in previous studies (Vieira, Garcia-Dias, & Pinaya, 2020).

The accuracy presented was obtained by averaging the values over all folds. The statistical significance of the overall classification accuracy was determined by conducting nonparametric permutation tests, which involve repeating the classification procedure 1,000 times with a different random permutation of the training group labels and counting the number of permutations achieving higher sensitivity and specificity than the true labels. Ultimately, a discriminative map was generated to display the relative contributions of each voxel to the SVM classification decision.

3 | RESULTS

3.1 | Demographic and clinical characteristics

The demographic information and clinical characteristics of all the subjects are presented in Table 1. No significant differences were identified with respect to sex ($p = 1.000$) or age ($p = .352$) between drug-naïve OCD patients and HCs. The mean ($\pm SD$) scores of the Y-BOCS, obsessions, compulsions, HAMD, and HAMA were 20.97 (± 5.26), 12.40 (± 4.44), 8.58 (± 5.34), 8.68 (± 5.28), and 9.16 (± 4.70), respectively. The illness duration of the OCD group was 7.47 ± 5.51 years, and the mean age of onset for patients was 22.23 years.

3.2 | Univariate results of group differences

Compared with HCs, patients with OCD showed increased dALFF in regions within CSTC circuits (i.e., the bilateral dorsal anterior cingulate cortex [dACC], medial prefrontal cortex [mPFC] and striatum [including the putamen and caudate], and the right dorsolateral prefrontal cortex [dlPFC]) and increased dALFF in the left MOG, inferior temporal gyrus, and MTG. Conversely, compared with HCs, OCD patients showed decreased dALFF in the bilateral inferior parietal lobule (IPL), posterior cingulate cortex (PCC), insula, fusiform gyrus, and cerebellum (Table 2 and Figure 1a).

We analyzed the data using different sliding window lengths (30 TRs and 80 TRs) and obtained similar results as the main finding, which is shown in Supplementary Figure S1.

In addition, we repeated our analysis with global signal regression, and the findings also revealed good consistency with the main results without global signal regression (Supplementary Figure S2).

3.3 | Relationship between dALFF and clinical symptoms

We found negative correlations between dALFF values in the right IPL and illness duration ($r = -.284; p = .015$; Figure 1b) and between

Characteristic	OCD (n = 73)		HCs (n = 73)		Significance	
	Mean	SD	Mean	SD	t/ χ^2	p
Sex (male: female)	43:30	—	43:30	—	0.000	1.000
Age (years)	29.70	8.51	28.19	10.84	0.934	.352
Illness duration (years)	7.47	5.51	—	—	—	—
Age of onset (years)	22.23	7.21	—	—	—	—
Y-BOCS total	20.97	5.26	—	—	—	—
Obsessions	12.40	4.44	—	—	—	—
Compulsions	8.58	5.34	—	—	—	—
HAMD 17	8.68	5.28	—	—	—	—
HAMA 14	9.16	4.70	—	—	—	—

TABLE 1 Demographic and clinical characteristics of drug-naïve OCD patients and HCs

Abbreviations: HAMA, Hamilton Anxiety Rating Scale; HAMD, Hamilton Depression Rating Scale; HCs, healthy control subjects; OCD, obsessive-compulsive disorder; SD, standard deviation; Y-BOCS, Yale-Brown Obsessive-Compulsive Scale.

dALFF values in the left cerebellum and HAMD scores ($r = -.28$; $p = .016$; Figure 1c). These results did not survive the FDR correction.

3.4 | Multivariate results from MVPA

The classification plots for the SVM classifier utilizing dALFF images are displayed in Figure 2a. The receiver operating characteristic curve evaluating the performance using dALFF as features is displayed in Figure 2b. The SVM yielded an accuracy of 83.56% for the comparison between OCD patients and HCs (sensitivity = 80.82%; specificity = 86.30%; $p = .001$).

The spatial maps of the brain regions that contributed to the discrimination between patients with OCD and HCs are shown in Figure 2c. These regions included the bilateral IPL, cuneus, left MOG, and right dIPFC.

3.5 | Reproducibility analysis

Split-half and leave-one-out methods were used to examine the reproducibility of the results of statistical comparisons (Li, Xu, Zhang, Hoptman, & Zuo, 2015; Zhang et al., 2011).

First, we divided the HC subjects into two subgroups matched for age and sex (HC1: 37 participants, 14 females, age: 29.00 ± 9.13 years; HC2: 36 participants, 16 females, age: 27.36 ± 12.44 years). Similarly, we divided the OCD patients into two subgroups (OCD1: 37 participants, 16 females, age: 29.38 ± 8.52 years; OCD2: 36 participants, 14 females, age: 30.03 ± 8.60 years) (all $p > .05$). We performed the same statistical comparisons between each HCs subgroups and OCD subgroups (i.e., HC1 vs. OCD1; HC1 vs. OCD2; HC2 vs. OCD1; HC2 vs. OCD2) as the full sample. The split-half results are shown in Figure 3a and basically replicated the findings from the full sample.

However, the group comparisons may significantly lose statistical power in the split-half analysis as the sample size was relatively small.

Therefore, we also performed leave-one-out method to validate the reproducibility and robustness of these results on dALFF without losing statistical power. Specifically, we left one OCD patient out of the sample and performed the same group comparisons based upon the permuted sample (i.e., 72 OCD vs. 73 HCs). This analysis led to a total of 73 two-sample *t*-test images, based on which, for each voxel, we calculated the number of tests where this voxel exhibited significant group differences across the 73 tests as the reproducibility of the dALFF differences between OCD patients and HCs. Leave-one-out sample validation suggested a highly reproducible pattern of dALFF across these tests as well as the original test (Figure 3b).

4 | DISCUSSION

To the best of our knowledge, the current study is the first to explore regional brain intrinsic activity fluctuations in a relatively large sample of drug-naïve patients with OCD. We demonstrated a characteristic pattern of dynamic changes for regional intrinsic activity in OCD patients with increased temporal variability mainly within CSTC circuits (i.e., the bilateral dACC, mPFC and striatum; and right dIPFC), while decreased dALFF was located outside of the CSTC regions, including the bilateral IPL, PCC, insula, fusiform gyrus and cerebellum. We also found that the dALFF in the right IPL correlated negatively with illness duration and that the dALFF in the left cerebellum correlated negatively with HAMD scores. Moreover, dALFF can distinguish OCD patients from HCs at the individual level with an accuracy of 83.56%, and the most discriminative regions were located mainly in the IPL, dIPFC, MOG, and cuneus.

The CSTC model of OCD (also termed the frontostriatal model or corticostriatal model) has been the prevailing model regarding the neural and pathophysiological underpinnings of OCD for years (Pauls, Abramovitch, Rauch, & Geller, 2014). It has three main components: affective circuits involving the ACC/ventral mPFC-nucleus accumbens-thalamus, dorsal cognitive circuits involving the dIPFC-caudate nucleus-thalamus and ventral cognitive circuits involving the orbitofrontal

TABLE 2 Significant differences in dALFF between drug-naïve OCD patients and HCs

Region	Side	Voxel size	MNI coordinate			T	p*
			x	y	z		
<i>OCD patients > HCs</i>							
Dorsolateral and medial prefrontal cortex, dorsal anterior cingulate cortex	L/R	1,650	36	30	-21	5.72	<.001
			-3	0	54	5.58	
			30	27	39	5.46	
Putamen, caudate	L	151	-27	12	-9	4.71	.006
			-21	18	-3	4.62	
			-24	6	9	4.25	
Putamen, caudate	R	107	27	15	-6	4.76	.016
			18	15	-9	4.10	
			15	18	9	3.99	
Middle occipital gyrus	L	319	-45	-81	18	6.11	<.001
			-54	-72	18	5.07	
			-36	-93	9	4.49	
Inferior temporal gyrus	L	302	-51	-30	-30	6.19	<.001
			-45	-36	-30	6.00	
			-42	-45	-39	5.07	
Middle temporal gyrus	L	147	-48	9	-27	4.72	.006
			-45	24	-15	4.42	
<i>OCD patients < HCs</i>							
Inferior parietal lobule	R	523	30	-60	45	-8.24	<.001
			36	-39	42	-6.06	
			30	-78	21	-4.89	
Inferior parietal lobule	L	163	-30	-51	42	-5.05	.004
			-48	-36	51	-4.81	
Cerebellum, fusiform gyrus	R	2,116	39	-72	-30	-7.70	<.001
			36	-72	-18	-7.34	
			21	-87	-21	-6.86	
Cerebellum, fusiform gyrus	L	330	-39	-75	-18	-5.30	<.001
			-24	-87	-15	-4.40	
			-27	-63	-18	-4.39	
Posterior cingulate cortex	L/R	176	12	-33	45	-4.20	.004
			-9	-39	45	-4.09	
			3	-45	51	-3.56	
Insula	R	89	39	-12	12	-4.25	.031
			36	-27	12	-4.15	
			57	-12	3	-3.68	
Insula	L	88	-33	-24	12	-4.82	.031
			-39	-9	0	-3.69	

Abbreviations: HCs, healthy control subjects; MNI, Montreal Neurological Institute; OCD, obsessive-compulsive disorder.

cortex-putamen-thalamus (Milad & Rauch, 2012). In the current study, we found increased dALFF in most of the above regions at the same time in OCD patients, providing direct evidence of the wide dysfunction in the CSTC circuits.

The dACC region is crucially involved in detecting the presence of cognitive conflicts, error monitoring, and detection in OCD (Melcher, Falkai, & Gruber, 2008; Milad & Rauch, 2012). The most consistent finding is hyperactivity in the region in OCD patients at

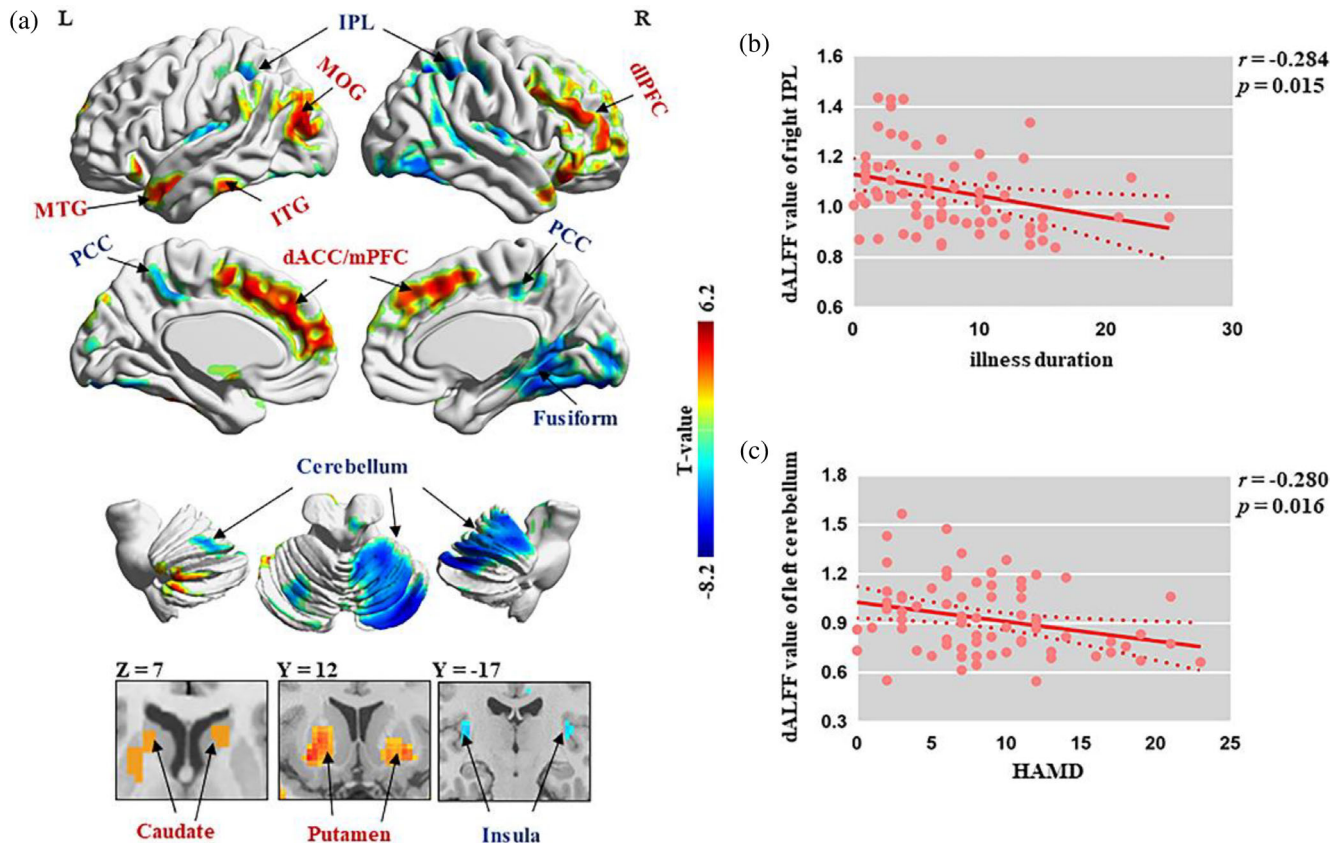


FIGURE 1 (a) Significant regions in the group comparison between OCD patients and HCs. Warm/cool colors indicate regions showing higher/lower dALFF values in the OCD group than in HCs. (b) Negative correlation between illness duration and dALFF values in the right IPL. (c) Negative correlation between HAMD and dALFF values in the left cerebellum. dACC, dorsal anterior cingulate cortex; dALFF, dynamic amplitude of low-frequency fluctuation; dIPFC, dorsolateral prefrontal cortex; HAMD, Hamilton Depression Rating Scale; HCs, healthy control subjects; IPL, inferior parietal lobule; ITG, inferior temporal gyrus; MOG, middle occipital gyrus; mPFC, medial prefrontal cortex; MTG, middle temporal gyrus; OCD, obsessive-compulsive disorder; PCC, posterior cingulate cortex

rest (Chen et al., 2019; Hou et al., 2012). Our study also showed overhyperactivity in the dACC, which may reflect abnormal error detection and conflict monitoring in OCD. OCD patients also exhibited greater activity in the mPFC than HCs due to a failure to deactivate this default mode network region (Stern et al., 2011), perhaps reflecting an inability of patients to disengage from automatic evaluative processes when errors occur (Bu et al., 2019). Additionally, prior studies reported that the striatum and dIPFC show increases in gray matter volume and activity in patients with OCD (Gao et al., 2019; Pico-Perez et al., 2020). Consistent with previous findings, the brain activity of the dACC, mPFC, striatum, and dIPFC displayed increased temporal variability in OCD patients, and the dIPFC also exhibited high discriminative power in the present study, providing further support for dysfunction in CSTC pathways in patients with OCD.

In addition to CSTC circuits, other models have implicated alterations in the frontoparietal, default mode, and salience networks (the triple network model), and the visual and cerebellar networks (Gürsel et al., 2018; Reggente et al., 2018; van den Heuvel et al., 2016). Interestingly, we found that OCD patients showed decreased dALFF in the bilateral IPL, PCC, insula, fusiform gyrus and cerebellum, supporting

the involvement of the above models and distinguishing their roles from CSTC circuits in the neural mechanism of OCD.

The IPL is the key region in the frontoparietal network involved in attention set shifting and response inhibition in OCD (Eng, Sim, & Chen, 2015). Patients with OCD showed decreased activity in the right IPL during inhibition relative to healthy comparison subjects, and a relationship was found between the activity in the IPL and stop-signal reaction time in the OCD group (de Wit et al., 2012). Similar to our results of decreased temporal variability in the IPL, a previous study also demonstrated hypoactivation in the right IPL during the resting state (Hou et al., 2012). Thus, the decreased regional activity of the IPL, as reflected by the dALFF in the current study, could reflect impaired attention to the stop signal or impaired action reprogramming, leading to excessive repetitive behavior.

Moreover, we discovered a negative correlation between dALFF values in the right IPL and illness duration in OCD patients, indicating that a longer illness duration is associated with decreased IPL function. This means that OCD is a progressive disease (Chen et al., 2016), and temporal variability changes in the right IPL may be a potential biomarker for the progression of OCD. However, as these correlations did not survive the FDR correction, thus the correlation results should

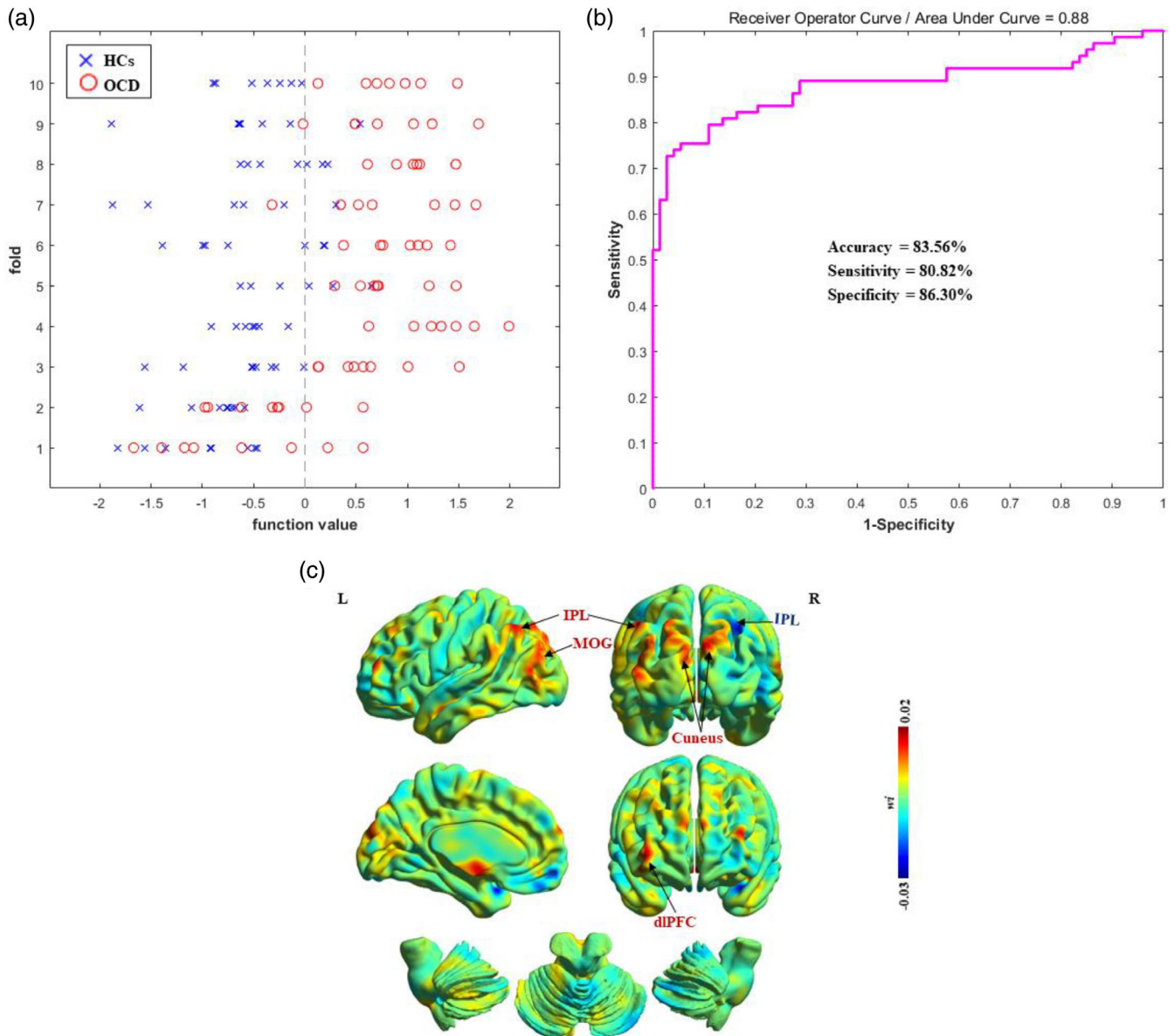


FIGURE 2 Classification performance for OCD patients and HCs. (a) Classification plots for the SVM classifier. (b) ROC curves assessing SVM performance. (c) Discrimination weight map using dALFF. The color bar indicates the weighted vector value determined from SVM. dALFF, dynamic amplitude of low-frequency fluctuation; dIPFC, dorsolateral prefrontal cortex; HCs, healthy control subjects; IPL, inferior parietal lobule; MOG, middle occipital gyrus; OCD, obsessive-compulsive disorder; ROC, receiver operating characteristic; SVM, support vector machine

be regard as preliminary and may need large sample of datasets to validate. The MVPA results suggest that the IPL is a major region with discriminative power and may be an important site for differentiating OCD patients from HCs at the individual level.

In addition to the frontoparietal network, we also found that the time-varying activity of hub regions in the default mode, salience, and visual networks was decreased in OCD patients. The PCC is a core region of the default mode network, and it controls the balance between internally and externally focused thoughts (Chen et al., 2019). The insula is a key hub in the salience network and is also related to internal and external stimulation. The region is important for switching attention away from an internal focus toward the

external environment after detecting potentially harmful situations (Stern et al., 2011). Studies have also displayed lower brain activity in these regions at rest in OCD patients than in HCs (Cheng et al., 2013; Zhu et al., 2016). Hypoactivity may suggest that patients have a decreased level of arousal and attention to external stimuli, likely explaining the immersion of OCD patients in their own intrusive thoughts and repetitive behaviors (Chen et al., 2019). Additionally, the fusiform gyrus is an important region in the visual network (Muthukrishnan, Soni, & Sharma, 2020) and is implicated in the visual processing dysfunction associated with OCD (Lei et al., 2020). The decreased dALFF in the fusiform gyrus in the present study may be associated with visual deficits in OCD.

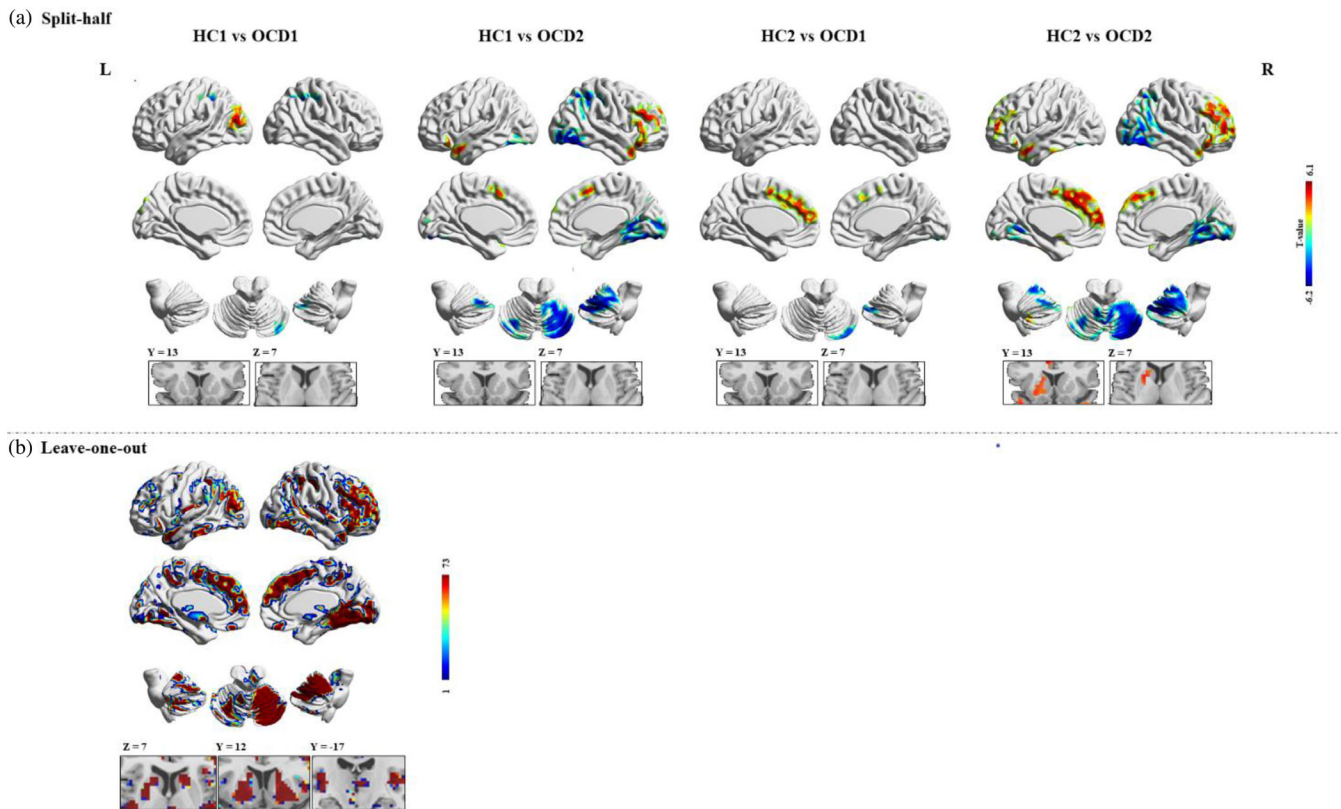


FIGURE 3 Reproducibility of dynamic amplitude of low-frequency fluctuation (dALFF) findings. (a) Split-half sample validation. For each voxel, the color indicates T scores of group comparison. (b) Leave-one-out sample validation. For each voxel, the color indicates the number of tests where this voxel exhibited significant group differences across the 73 tests

We also found reduced temporal variability in the bilateral cerebellum in OCD patients compared with HCs, and it was also associated with increased depressive symptoms, as revealed by HAMD scores. The cerebellar network is another part outside the CSTC network. An increasing number of studies have reported that, in addition to the traditional role of motor control, the primate cerebellum is involved in cognitive control and emotional regulation (Hu et al., 2019). Furthermore, the cerebellum has also been implicated in ruminative and obsessive behaviors (Figeo, Wielaard, Mazaheri, & Denys, 2013; Schmahmann, Weilburg, & Sherman, 2007), which are related to OCD. Most previous rs-fMRI studies have shown decreased intrinsic activity in the cerebellum in OCD patients (Hou et al., 2012; Qiu et al., 2017), the finding that is consistent with ours. OCD symptoms typically precede the onset of depressive symptoms (Jones, Mair, Riemann, Mugno, & McNally, 2018), and distress related to obsessional thoughts and concentration problems link depressive and OCD symptom clusters (Sha et al., 2020). Thus, the negative correlation between the cerebellum and HAMD scores in our study might reflect a relationship between the cerebellum and cognitive dysfunction in OCD.

We found that dALFF had a relative higher accuracy in distinguishing OCD from HCs compared with most previous studies. For example, a study achieved 72% accuracy using fractional ALFF of 68 drug-naïve OCD patients and 68 HCs (Yang et al., 2019), another

study got 78.98% accuracy using regional homogeneity of 88 medication-free OCD patients and 88 HCs (Hu et al., 2019). A seed-based resting state functional connectivity revealed that the abnormal cerebellar-default mode network connectivity can be used to discriminate patients with OCD from HCs with an accuracy of 76.92% (Lv et al., 2020). In our current study, OCD patients could be differentiated from HCs based on dALFF with classification accuracy of 83.56%, though our previous study with smaller sample size showed a higher accuracy of 95.37% for discriminating drug-naïve OCD from HCs using ALFF (Bu et al., 2019). We suppose that the lower classification accuracy of dALFF compared with ALFF maybe represents less sensitivity of distinguishing OCD patients from HCs in our population, and this raises the necessity of evaluating different parameters in different datasets for translational purpose.

A few limitations in the current study are worth mentioning. First, our results were from drug-naïve OCD patients, providing more direct evidence of the intrinsic function of the brain relevant to the disease itself without confounding factors of medication; however, our results may not apply to other OCD populations such as those who had been on medication for years. Future work will be necessary to explore the time-varying intrinsic brain activity in other OCD populations. Second, the selection of the optimal sliding window length for obtaining the dynamics of brain activity remains unclear. We selected 50 TRs as the window length based on previous studies. We validated our

results by utilizing different sliding window lengths and demonstrated that our findings are stable and not substantially influenced by this factor. Third, patients with different subtypes or experiencing different level of childhood trauma would exhibit different neural alterations. However, due to the lack of those information, we cannot explore the impact of these factors in current study. Fourth, the group comparison of some confounding factors such as education duration or socioeconomic status is not clear due to the lack of relevant information. This may have a little impact on the results of the group comparison.

5 | CONCLUSIONS

In summary, we demonstrated characteristic changes in increased dynamic intrinsic activity in CSTC circuits and decreased variability in regions outside of the circuits in OCD patients. In particular, we emphasize that the dysfunction of regions outside the CSTC circuits, such as the parietal cortex and cerebellum, plays an important role in the pathophysiology of OCD. Furthermore, the SVM analysis of dALFF achieved the accuracy of 83.56% in classifying OCD patients and HCs at the individual level, with different CV strategies showing similar accuracy, which indicated the stability of results achieved in the current study.

ACKNOWLEDGMENTS

The authors would like to thank their tutor and colleagues for their time and valuable help. This study was supported by the National Natural Science Foundation (grant No. 81671669), Science and Technology Project of Sichuan Province (grant No. 2017JQ0001) and Science and Technology Project of Chengdu City (grant No. 2019-YF05-00509-SN).

CONFLICT OF INTERESTS

The authors declare no conflicts of interest.

DATA AVAILABILITY STATEMENT

The data that support the findings of this study are available from the corresponding author upon reasonable request.

ORCID

Qiyong Gong  <https://orcid.org/0000-0002-5912-4871>

Xiaoqi Huang  <https://orcid.org/0000-0001-8686-5010>

REFERENCES

- Aiello, M., Salvatore, E., Cachia, A., Pappatà, S., Cavaliere, C., Prinster, A., ... Quarantelli, M. (2015). Relationship between simultaneously acquired resting-state regional cerebral glucose metabolism and functional MRI: A PET/MR hybrid scanner study. *NeuroImage*, 113, 111–121. <https://doi.org/10.1016/j.neuroimage.2015.03.017>
- Ashburner, J. (2007). A fast diffeomorphic image registration algorithm. *NeuroImage*, 38(1), 95–113. <https://doi.org/10.1016/j.neuroimage.2007.07.007>
- Ashburner, J., Chu, C., Marquand, A., Mourao-Miranda, J., Monteiro, J. M., Phillips, C., ... Schrouff, J. (2012). The PRoNTo development group.
- Benedetti, F., Giacosa, C., Radaelli, D., Poletti, S., Pozzi, E., Dallspezia, S., ... Smeraldi, E. (2013). Widespread changes of white matter microstructure in obsessive-compulsive disorder: Effect of drug status. *European Neuropsychopharmacology*, 23(7), 581–593. <https://doi.org/10.1016/j.euroneuro.2012.07.002>
- Boedhoe, P. S. W., Schmaal, L., Abe, Y., Alonso, P., Ameis, S. H., Anticevic, A., ... Grp, E.-O. W. (2018). Cortical abnormalities associated with pediatric and adult obsessive-compulsive disorder: Findings from the ENIGMA obsessive-compulsive disorder working group. *American Journal of Psychiatry*, 175(5), 453–462. <https://doi.org/10.1176/appi.ajp.2017.17050485>
- Bu, X., Hu, X., Zhang, L., Li, B., Zhou, M., Lu, L., ... Huang, X. (2019). Investigating the predictive value of different resting-state functional MRI parameters in obsessive-compulsive disorder. *Translational Psychiatry*, 9(1), 17. <https://doi.org/10.1038/s41398-018-0362-9>
- Chen, Y., Meng, X., Hu, Q., Cui, H., Ding, Y., Kang, L., ... Li, P. (2016). Altered resting-state functional organization within the central executive network in obsessive-compulsive disorder. *Psychiatry and Clinical Neurosciences*, 70(10), 448–456. <https://doi.org/10.1111/pcn.12419>
- Chen, Y., Ou, Y., Lv, D., Yang, R., Li, S., Jia, C., ... Li, P. (2019). Altered network homogeneity of the default-mode network in drug-naïve obsessive-compulsive disorder. *Progress in Neuro-Psychopharmacology & Biological Psychiatry*, 93, 77–83. <https://doi.org/10.1016/j.pnpbbp.2019.03.008>
- Cheng, Y., Xu, J., Nie, B., Luo, C., Yang, T., Li, H., ... Xu, X. (2013). Abnormal resting-state activities and functional connectivities of the anterior and the posterior cortexes in medication-naïve patients with obsessive-compulsive disorder. *PLoS One*, 8(6), e67478. <https://doi.org/10.1371/journal.pone.0067478>
- Cui, Q., Sheng, W., Chen, Y., Pang, Y., Lu, F., Tang, Q., ... Chen, H. (2020). Dynamic changes of amplitude of low-frequency fluctuations in patients with generalized anxiety disorder. *Human Brain Mapping*, 41(6), 1667–1676. <https://doi.org/10.1002/hbm.24902>
- de Wit, S. J., de Vries, F. E., van der Werf, Y. D., Cath, D. C., Heslenfeld, D. J., Veltman, E. M., ... van den Heuvel, O. A. (2012). Presupplementary motor area hyperactivity during response inhibition: A candidate endophenotype of obsessive-compulsive disorder. *American Journal of Psychiatry*, 169(10), 1100–1108. <https://doi.org/10.1176/appi.ajp.2012.12010073>
- Denkova, E., Nomi, J. S., Uddin, L. Q., & Jha, A. P. (2019). Dynamic brain network configurations during rest and an attention task with frequent occurrence of mind wandering. *Human Brain Mapping*, 40(15), 4564–4576. <https://doi.org/10.1002/hbm.24721>
- Eng, G. K., Sim, K., & Chen, S. H. (2015). Meta-analytic investigations of structural grey matter, executive domain-related functional activations, and white matter diffusivity in obsessive compulsive disorder: An integrative review. *Neuroscience & Biobehavioral Reviews*, 52, 233–257. <https://doi.org/10.1016/j.neubiorev.2015.03.002>
- Fan, J., Zhong, M., Gan, J., Liu, W., Niu, C., Liao, H., ... Zhu, X. (2017). Spontaneous neural activity in the right superior temporal gyrus and left middle temporal gyrus is associated with insight level in obsessive-compulsive disorder. *Journal of Affective Disorders*, 207, 203–211. <https://doi.org/10.1016/j.jad.2016.08.027>
- Figure, M., Wiersma, I., Mazaheri, A., & Denys, D. (2013). Neurosurgical targets for compulsivity: What can we learn from acquired brain lesions? *Neuroscience & Biobehavioral Reviews*, 37(3), 328–339. <https://doi.org/10.1016/j.neubiorev.2013.01.005>
- Friston, K. J., Williams, S., Howard, R., Frackowiak, R. S., & Turner, R. (1996). Movement-related effects in fMRI time-series. *Magnetic Resonance in Medicine*, 35(3), 346–355. <https://doi.org/10.1002/mrm.1910350312>
- Fu, Z. N., Tu, Y. H., Di, X., Du, Y. H., Pearson, G. D., Turner, J. A., ... Calhoun, V. D. (2018). Characterizing dynamic amplitude of low-frequency fluctuation and its relationship with dynamic functional

- connectivity: An application to schizophrenia. *NeuroImage*, 180(Pt B), 619–631. <https://doi.org/10.1016/j.neuroimage.2017.09.035>
- Gao, J., Zhou, Y., Yang, X., Luo, J., Meng, F., Zheng, D., & Li, Z. (2019). Abnormalities within and beyond the cortico-striato-thalamo-cortical circuitry in medication-free patients with OCD revealed by the fractional amplitude of low-frequency fluctuations and resting-state functional connectivity. *Neuroscience Letters*, 712, 134449. <https://doi.org/10.1016/j.neulet.2019.134449>
- Gürsel, D. A., Avram, M., Sorg, C., Brandl, F., & Koch, K. (2018). Frontoparietal areas link impairments of large-scale intrinsic brain networks with aberrant fronto-striatal interactions in OCD: A meta-analysis of resting-state functional connectivity. *Neuroscience & Biobehavioral Reviews*, 87, 151–160. <https://doi.org/10.1016/j.neubiorev.2018.01.016>
- Gürsel, D. A., Reinholz, L., Bremer, B., Schmitz-Koep, B., Franzmeier, N., Avram, M., & Koch, K. (2020). Frontoparietal and salience network alterations in obsessive-compulsive disorder: Insights from independent component and sliding time window analyses. *Journal of Psychiatry & Neuroscience*, 45(3), 214–221. <https://doi.org/10.1503/jpn.190038>
- Halai, A. D., Woollams, A. M., & Lambon Ralph, M. A. (2020). Investigating the effect of changing parameters when building prediction models for post-stroke aphasia. *Nature Human Behaviour*, 4(7), 725–735. <https://doi.org/10.1038/s41562-020-0854-5>
- Hou, J., Wu, W., Lin, Y., Wang, J., Zhou, D., Guo, J., ... Li, H. (2012). Localization of cerebral functional deficits in patients with obsessive-compulsive disorder: A resting-state fMRI study. *Journal of Affective Disorders*, 138(3), 313–321. <https://doi.org/10.1016/j.jad.2012.01.022>
- Hou, J.-M., Zhao, M., Zhang, W., Song, L.-H., Wu, W.-J., Wang, J., ... Guo, J.-W. (2014). Resting-state functional connectivity abnormalities in patients with obsessive-compulsive disorder and their healthy first-degree relatives. *Journal of Psychiatry & Neuroscience*, 39(5), 304–311. <https://doi.org/10.1503/jpn.130220>
- Hu, X., Zhang, L., Bu, X., Li, H., Li, B., Tang, W., ... Huang, X. (2019). Localized connectivity in obsessive-compulsive disorder: An investigation combining univariate and multivariate pattern analyses. *Frontiers in Behavioral Neuroscience*, 13, 122. <https://doi.org/10.3389/fnbeh.2019.00122>
- Huang, X., Gong, Q., Sweeney, J. A., & Biswal, B. B. (2019). Progress in psychoradiology, the clinical application of psychiatric neuroimaging. *The British Institute of Radiology*, 92(1101), 20181000. <https://doi.org/10.1259/bjr.20181000>
- Jenkinson, M., Bannister, P., Brady, M., & Smith, S. (2002). Improved optimization for the robust and accurate linear registration and motion correction of brain images. *NeuroImage*, 17(2), 825–841. [https://doi.org/10.1016/s1053-8119\(02\)91132-8](https://doi.org/10.1016/s1053-8119(02)91132-8)
- Jones, P. J., Mair, P., Riemann, B. C., Mugno, B. L., & McNally, R. J. (2018). A network perspective on comorbid depression in adolescents with obsessive-compulsive disorder. *Journal of Anxiety Disorders*, 53, 1–8. <https://doi.org/10.1016/j.janxdis.2017.09.008>
- Lei, H., Huang, L., Li, J., Liu, W., Fan, J., Zhang, X., ... Rao, H. (2020). Altered spontaneous brain activity in obsessive-compulsive personality disorder. *Comprehensive Psychiatry*, 96, 152144. <https://doi.org/10.1016/j.comppsy.2019.152144>
- Li, H. J., Xu, Y., Zhang, K. R., Hoptman, M. J., & Zuo, X. N. (2015). Homotopic connectivity in drug-naïve, first-episode, early-onset schizophrenia. *The Journal of Child Psychology and Psychiatry*, 56(4), 432–443. <https://doi.org/10.1111/jcpp.12307>
- Liao, W., Li, J., Ji, G. J., Wu, G. R., Long, Z. L., Xu, Q., ... Chen, H. F. (2019). Endless fluctuations: Temporal dynamics of the amplitude of low frequency fluctuations. *IEEE Transactions on Medical Imaging*, 38(11), 2523–2532. <https://doi.org/10.1109/Tmi.2019.2904555>
- Liao, W., Wang, J., Xu, T., Zhang, Z., Ji, G.-J., Xu, Q., ... Qiu, A. (2016). Altered relationship between thickness and intrinsic activity amplitude in generalized tonic-clonic seizures. *Science Bulletin*, 61(24), 1865–1875. <https://doi.org/10.1007/s11434-016-1201-0>
- Liu, J., Li, X., Xue, K., Chen, Y., Wang, K., Niu, Q., ... Cheng, J. (2020). Abnormal dynamics of functional connectivity in first-episode and treatment-naïve patients with obsessive-compulsive disorder. *Psychiatry and Clinical Neurosciences*, 75, 14–22. <https://doi.org/10.1111/pcn.13162>
- Lv, D., Ou, Y., Chen, Y., Yang, R., Zhong, Z., Jia, C., ... Li, P. (2020). Increased cerebellar-default-mode network connectivity at rest in obsessive-compulsive disorder. *European Archives of Psychiatry and Clinical Neuroscience*, 270(8), 1015–1024. <https://doi.org/10.1007/s00406-019-01070-5>
- Melcher, T., Falkai, P., & Gruber, O. (2008). Functional brain abnormalities in psychiatric disorders: Neural mechanisms to detect and resolve cognitive conflict and interference. *Brain Research Reviews*, 59(1), 96–124. <https://doi.org/10.1016/j.brainresrev.2008.06.003>
- Milad, M. R., & Rauch, S. L. (2012). Obsessive-compulsive disorder: Beyond segregated cortico-striatal pathways. *Trends in Cognitive Sciences*, 16(1), 43–51. <https://doi.org/10.1016/j.tics.2011.11.003>
- Muthukrishnan, S. P., Soni, S., & Sharma, R. (2020). Brain networks communicate through theta oscillations to encode high load in a visuospatial working memory task: An EEG connectivity study. *Brain Topography*, 33(1), 75–85. <https://doi.org/10.1007/s10548-019-00739-3>
- Pauls, D. L., Abramovitch, A., Rauch, S. L., & Geller, D. A. (2014). Obsessive-compulsive disorder: An integrative genetic and neurobiological perspective. *Nature Reviews Neuroscience*, 15(6), 410–424. <https://doi.org/10.1038/nrn3746>
- Pico-Perez, M., Moreira, P. S., de Melo Ferreira, V., Radua, J., Mataix-Cols, D., Sousa, N., ... Morgado, P. (2020). Modality-specific overlaps in brain structure and function in obsessive-compulsive disorder: Multimodal meta-analysis of case-control MRI studies. *Neuroscience & Biobehavioral Reviews*, 112, 83–94. <https://doi.org/10.1016/j.neubiorev.2020.01.033>
- Power, J. D., Barnes, K. A., Snyder, A. Z., Schlaggar, B. L., & Petersen, S. E. (2013). Steps toward optimizing motion artifact removal in functional connectivity MRI; a reply to carp. *NeuroImage*, 76, 439–441. <https://doi.org/10.1016/j.neuroimage.2012.03.017>
- Qiu, L., Fu, X., Wang, S., Tang, Q., Chen, X., Cheng, L., ... Tian, L. (2017). Abnormal regional spontaneous neuronal activity associated with symptom severity in treatment-naïve patients with obsessive-compulsive disorder revealed by resting-state functional MRI. *Neuroscience Letters*, 640, 99–104. <https://doi.org/10.1016/j.neulet.2017.01.024>
- Qiu, L., Xia, M., Cheng, B., Yuan, L., Kuang, W., Bi, F., ... Gong, Q. (2018). Abnormal dynamic functional connectivity of amygdalar subregions in untreated patients with first-episode major depressive disorder. *Journal of Psychiatry & Neuroscience*, 43(4), 262–272. <https://doi.org/10.1503/jpn.170112>
- Raichle, M. E., & Snyder, A. Z. (2007). A default mode of brain function: A brief history of an evolving idea. *NeuroImage*, 37(4), 1083–1090. <https://doi.org/10.1016/j.neuroimage.2007.02.041>
- Reggente, N., Moody, T. D., Morfini, F., Sheen, C., Rissman, J., O'Neill, J., & Feusner, J. D. (2018). Multivariate resting-state functional connectivity predicts response to cognitive behavioral therapy in obsessive-compulsive disorder. *Proceedings of the National Academy of Sciences of the United States of America*, 115(9), 2222–2227. <https://doi.org/10.1073/pnas.1716686115>
- Satterthwaite, T. D., Elliott, M. A., Gerraty, R. T., Ruparel, K., Loughhead, J., Calkins, M. E., ... Wolf, D. H. (2013). An improved framework for confound regression and filtering for control of motion artifact in the preprocessing of resting-state functional connectivity data. *NeuroImage*, 64, 240–256. <https://doi.org/10.1016/j.neuroimage.2012.08.052>
- Schmahmann, J. D., Weilburg, J. B., & Sherman, J. C. (2007). The neuropsychiatry of the cerebellum—Insights from the clinic. *Cerebellum*, 6(3), 254–267. <https://doi.org/10.1080/14734220701490995>

- Schrouff, J., Mourão-Miranda, J., Phillips, C., & Parvizi, J. (2016). Decoding intracranial EEG data with multiple kernel learning method. *Journal of Neuroscience Methods*, 261, 19–28. <https://doi.org/10.1016/j.jneumeth.2015.11.028>
- Sha, Z. Q., Versace, A., Edmiston, E. K., Fournier, J., Graur, S., Greenberg, T., ... Phillips, M. L. (2020). Functional disruption in prefrontal-striatal network in obsessive-compulsive disorder. *Psychiatry Research: Neuroimaging*, 300, 111081. <https://doi.org/10.1016/j.psychres.2020.111081>
- Stein, D. J., Costa, D. L. C., Lochner, C., Miguel, E. C., Reddy, Y. C. J., Shavitt, R. G., ... Simpson, H. B. (2019). Obsessive-compulsive disorder. *Nature Reviews Disease Primers*, 5(1), 52. <https://doi.org/10.1038/s41572-019-0102-3>
- Stern, E. R., Welsh, R. C., Fitzgerald, K. D., Gehring, W. J., Lister, J. J., Himle, J. A., ... Taylor, S. F. (2011). Hyperactive error responses and altered connectivity in ventromedial and frontoinsula cortices in obsessive-compulsive disorder. *Biological Psychiatry*, 69(6), 583–591. <https://doi.org/10.1016/j.biopsych.2010.09.048>
- van den Heuvel, O. A., van Wingen, G., Soriano-Mas, C., Alonso, P., Chamberlain, S. R., Nakamae, T., ... Veltman, D. J. (2016). Brain circuitry of compulsivity. *European Neuropsychopharmacology*, 26(5), 810–827. <https://doi.org/10.1016/j.euroneuro.2015.12.005>
- Vieira, S., Garcia-Dias, R., & Pinaya, W. H. L. (2020). Chapter 19 - A step-by-step tutorial on how to build a machine learning model. In *Machine learning* (pp. 343–370). Cambridge, MA: Academic Press.
- Vieira, S., Pinaya, W. H. L., & Mechelli, A. (2017). Using deep learning to investigate the neuroimaging correlates of psychiatric and neurological disorders: Methods and applications. *Neuroscience and Biobehavioral Reviews*, 74(Pt A), 58–75. <https://doi.org/10.1016/j.neubiorev.2017.01.002>
- Wang, X., Zhang, W., Sun, Y., Hu, M., & Chen, A. (2016). Aberrant intrasaliency network dynamic functional connectivity impairs large-scale network interactions in schizophrenia. *Neuropsychologia*, 93(Pt A), 262–270. <https://doi.org/10.1016/j.neuropsychologia.2016.11.003>
- Xu, T., Zhao, Q., Wang, P., Fan, Q., Chen, J., Zhang, H., ... Wang, Z. (2019). Altered resting-state cerebellar-cerebral functional connectivity in obsessive-compulsive disorder. *Psychological Medicine*, 49(7), 1156–1165. <https://doi.org/10.1017/s0033291718001915>
- Yan, C. G., Cheung, B., Kelly, C., Colcombe, S., Craddock, R. C., di Martino, A., ... Milham, M. P. (2013). A comprehensive assessment of regional variation in the impact of head micromovements on functional connectomics. *NeuroImage*, 76(1), 183–201. <https://doi.org/10.1016/j.neuroimage.2013.03.004>
- Yan, C. G., Wang, X. D., Zuo, X. N., & Zang, Y. F. (2016). DPABI: Data processing and analysis for (resting-state) brain imaging. *Neuroinformatics*, 14(3), 339–351. <https://doi.org/10.1007/s12021-016-9299-4>
- Yan, C.-G., Yang, Z., Colcombe, S. J., Zuo, X.-N., & Milham, M. P. (2017). Concordance among indices of intrinsic brain function: Insights from inter-individual variation and temporal dynamics. *Science Bulletin*, 62(23), 1572–1584. <https://doi.org/10.1016/j.scib.2017.09.015>
- Yang, X., Hu, X., Tang, W., Li, B., Yang, Y., Gong, Q., & Huang, X. (2019). Multivariate classification of drug-naïve obsessive-compulsive disorder patients and healthy controls by applying an SVM to resting-state functional MRI data. *BMC Psychiatry*, 19(1), 210. <https://doi.org/10.1186/s12888-019-2184-6>
- Yin, D., Zhang, C., Lv, Q., Chen, X., Zeljic, K., Gong, H., ... Sun, B. (2018). Dissociable frontostriatal connectivity: Mechanism and predictor of the clinical efficacy of capsulotomy in obsessive-compulsive disorder. *Biological Psychiatry*, 84(12), 926–936. <https://doi.org/10.1016/j.biopsych.2018.04.006>
- Youssofzadeh, V., McGuinness, B., Maguire, L. P., & Wong-Lin, K. (2017). Multi-kernel learning with DARTEL improves combined MRI-PET classification of Alzheimer's disease in AIBL data: Group and individual analyses. *Frontiers in Human Neuroscience*, 11, 380. <https://doi.org/10.3389/fnhum.2017.00380>
- Zang, Y. F., He, Y., Zhu, C. Z., Cao, Q. J., Sui, M. Q., Liang, M., ... Wang, Y. F. (2007). Altered baseline brain activity in children with ADHD revealed by resting-state functional MRI. *Brain and Development*, 29(2), 83–91. <https://doi.org/10.1016/j.braindev.2006.07.002>
- Zhang, Z., Liao, W., Chen, H., Mantini, D., Ding, J. R., Xu, Q., ... Lu, G. (2011). Altered functional-structural coupling of large-scale brain networks in idiopathic generalized epilepsy. *Brain*, 134(Pt 10), 2912–2928. <https://doi.org/10.1093/brain/awr223>
- Zhu, Y., Fan, Q., Zhang, H., Qiu, J., Tan, L., Xiao, Z., ... Li, Y. (2016). Altered intrinsic insular activity predicts symptom severity in unmedicated obsessive-compulsive disorder patients: A resting state functional magnetic resonance imaging study. *BMC Psychiatry*, 16, 104. <https://doi.org/10.1186/s12888-016-0806-9>

SUPPORTING INFORMATION

Additional supporting information may be found online in the Supporting Information section at the end of this article.

How to cite this article: Liu, J., Bu, X., Hu, X., Li, H., Cao, L., Gao, Y., Liang, K., Zhang, L., Lu, L., Hu, X., Wang, Y., Gong, Q., & Huang, X. (2021). Temporal variability of regional intrinsic neural activity in drug-naïve patients with obsessive-compulsive disorder. *Human Brain Mapping*, 42(12), 3792–3803. <https://doi.org/10.1002/hbm.25465>